Point contact Andreev reflection from semimetallic bismuth—The roles of the minority carriers and the large spin-orbit coupling

P. Stamenov

Citation: Journal of Applied Physics **113**, 17C718 (2013); doi: 10.1063/1.4796049
View online: http://dx.doi.org/10.1063/1.4796049
View Table of Contents: http://scitation.aip.org/content/aip/journal/jap/113/17?ver=pdfcov
Published by the AIP Publishing

Point contact Andreev reflection from semimetallic bismuth—The roles of the minority carriers and the large spin-orbit coupling

P. Stamenov[a)]
School of Physics and CRANN, Trinity College, Dublin 2, Ireland

(Presented 17 January 2013; received 9 November 2012; accepted 18 December 2012; published online 27 March 2013)

The Point Contact Andreev Reflection (PCAR) technique has been traditionally and predominantly applied to either the characterisation of superconductors or of spin-polarised metals. The sufficiently large and slowly varying, on the scale of tens of meV around the Fermi level (E_F), Density of States (DOS) in metals and highly degenerate semiconductors significantly simplifies the interpretation and quantitative analysis of the measured Differential Conductance Spectra (DCS). Semimetals in general, and particularly the heavy semimetals, because of the presence of several carrier bands and the larger Spin-Orbit coupling, exhibit significantly higher variations in the DOS, close to E_F, which can be observed and evaluated with PCAR. Here, DCS of bismuth/niobium point contacts are examined to reveal the relative energy offsets [0.12(3), 2.32(5), and 5.7(2)] meV and the approximate relative DOS contributions of the three main carrier bands (16:5:4). Apart from the bulk, some surface states are also expected to contribute to the observed DOS and be potentially spin-split. The spin polarisation due to all conducting states is evaluated at $P \leq 0.09(7)$. © *2013 American Institute of Physics*. [http://dx.doi.org/10.1063/1.4796049]

Bismuth is an important example of a heavy, large spin-orbit (SO) coupling semimetal, and the elemental conductor with the highest magnetoresistance coefficients. Together with its light counterpart, graphite, it has been instrumental to the development of both experimental and theoretical Fermi surface characterisation techniques.[1] Despite the strong diamagnetism of bulk Bi, there have been both theoretical and experimental efforts[2] towards the understanding of the influence of the large SO coupling on the spin-splitting of the minority carrier bands and, of some surface states. Here, polycrystalline Bi is investigated, utilizing the real-time Point Contact Andreev Reflection (PCAR) methodology, described elsewhere.[3] It is suggested that the same may be applicable to the characterisation of the electronic structure of other semimetals, such as graphite. The PCAR methodology has been extensively utilised for the evaluation of the Fermi level spin polarisation in magnetic metals.[4] The quantity extracted, in most practical cases, is $|P|$, and is defined as: $P = \frac{\langle D_\uparrow v_\uparrow^2\rangle - \langle D_\downarrow v_\downarrow^2\rangle}{\langle D_\uparrow v_\uparrow^2\rangle + \langle D_\downarrow v_\downarrow^2\rangle}$, where $D_\updownarrow$ is the spin polarised (and energy dependent) density of states (DOS) and $v_\updownarrow$ is the electronic velocity. The angle brackets imply diffusive averaging over energy and momentum, which is a common and useful case. Details about the nature of the averaging and the appropriate definitions of spin polarisation, to other types of experimental methods, can be found in Ref. 5. PCAR has also been exploited to characterise the quasi-particle DOS and the scattering processes with novel superconductors (see Refs. 6 and 7), but has not yet been adopted to the characterisation of semimetals.

The bismuth sample studied is prepared by mechanically polishing a face on a small 4N5 purity Bi ingot, subsequently etching in dilute sulphuric and nitric acids and finally lapping the surface with diamond-loaded polymer film (<0.3 μm grain size) under isopropanol, in order to avoid excessive oxidation, and transferred into the experimental cryostat (<1 mbar of He) under liquid. The acid etch has revealed crystallite size of about 100 μm, well above the radius of curvature of the shear-cut niobium tips used (30 nm-1 μm), ensuring that only one crystal face is likely to be addressed with any given contact.

The experiments are performed at lattice temperatures from 1.8 to 15 K in a He vapour-flow through sample space cryostat (Oxford instruments). Magnetic field is applied by a "Multimag" permanent-magnet-based variable-flux source, capable of providing up to $\mu_0 H = 1$ T, in any direction within the plane normal to the dominant current direction. At nominal zero field, the uncompensated magnetic field components at the sample are smaller than 0.5 mT. The translation of the superconducting tip with respect to the sample, necessary for the formation of the point contacts, is provided by a differential micrometer drive and a single-axis piezo positioner. The basics of the setup are similar to the ones described in Ref. 8 and the real-time Differential Conductance Spectra (DCS) measurement system, and the spectral fitting software are all updated versions of the ones described previously.[3] The modelling of the conventional PCAR spectra is based on the well-known modified BTK[9] theory, further taking into account superconducting proximity, electronic heating, modulation broadening, and series resistance. Least squares fitting of most of the experimental data is performed using fixed closed interval difference norm minimisation procedures, already described elsewhere.[10] Large variety of contacts are formed to the same sample surface and the contact exhibiting the largest evaluated polarisation P is taken as representative (in this case, the vast majority of the contact data refine to vanishingly

a)Electronic mail: stamenov.plamen@tcd.ie

small spin polarisation P). No extrapolations, such as the ones described in Ref. 11, have been performed, thus evaluating P at the pessimistic limit, with respect to most systematic errors. The uncertainties of the derived parameters are evaluated, following the conventional approach of computing the Jacobian derivative matrix $\mathbf{J}$, with respect to all fitting parameters and the data vector of the applied bias, using an iterative procedure with guarantied maximal error of the evaluation of 1% of the smallest value; then using $\mathbf{J}$ to compute the covariance matrix $\mathbf{C} = (\mathbf{J}^{\mathrm{T}}.\mathbf{J})^{-1}$, as its concatenation; and finally computing the standard absolute errors as $\sqrt{\mathrm{diag}(\sigma.\mathbf{C})}$, where σ is the reduced, normalized difference function χ^2. The resulting error is further corrected using Student's t-distribution, and has been shown to be well-behaved for a well-constructed (non-underdetermined) PCAR fitting model (see, for example, Ref. 3).

Contact size can be controlled by varying contact pressure (see, for example, Fig. 1), however, this is not always a monotonic process, and contact rearrangement and relaxation does occur often (especially in cases of relatively ductile samples). In the majority of cases, the contacts contain a single weak link, until a situation is reached (usually at the end-of-life of the Nb tip), when the junctions formed contain two or more discrete point contacts.[12] For the purposes of this analysis, these have been excluded from presented set, despite the fact that some of these are actually interpretable within more complicated fitting models (see Ref. 10). It is profiles, as the one in Fig. 1, that allow for the discrimination between close-to-ballistic (where the DCS features tend to keep their bias locations) and diffusive contacts (where DCS features tend to "creep" to higher biases). Some of the DCS observed at the initial stages of contact formation (see Fig. 2) are not interpretable within the same conventional framework [within the approximation that the DOS is constant in the useful bias region, which is limited experimentally to about $3\Delta_2 - 7\Delta_2$ (where $\Delta_2 \sim 1.5$ meV for Nb, is the bulk supercond. gap) depending primarily on the lateral size of the contact, by critical current artefacts.[13] These spectra are believed to be strongly influenced by the variations in the DOS close to E_{F} in semimetallic normal conductors (bismuth and graphite are two common examples). Indeed, the electronic current is proportional to the DOS on both sides

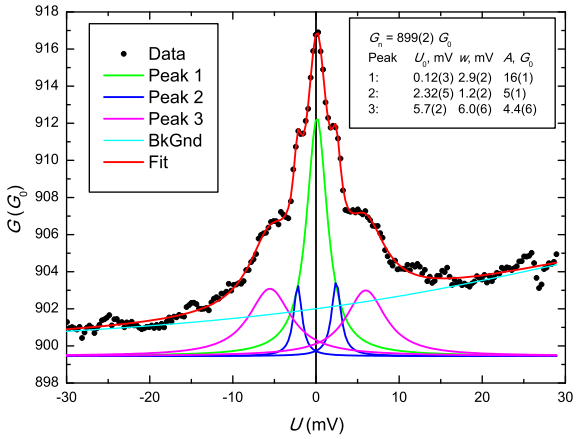

FIG. 2. PCAR spectrum of a high conductance Nb/Bi contact at $T = 2.5$ K and $\mu_0 H = 0.0$ mT, and the corresponding fit assuming three carrier bands contributing close to E_{F}.

of the contact $I \propto \int N_{\mathrm{L}}(E) N_{\mathrm{R}}(E - qV)[f(E - qV) - f(E)]\,\mathrm{d}E$, where $N_{\mathrm{L,R}}$ is the DOS of the left/right side, V is the applied bias, and f is the Fermi distribution function, independently of whether the transfer Hamiltonian or the Bogoliubov approach for computing it is taken (see, for example, Ref. 9). In similar cases, the small and non-trivial DOS can be taken to be the dominant factor, and the interpretation of the spectra is performed by fitting a number of Lorentzian peaks, each associated with the edge of a particular carrier band, using conventional non-linear least squares regression.

The majority of the observed PCAR spectra can be interpreted as characteristic to high interfacial barrier contacts with $Z > 0.2$, strong suppression of the quasiparticle gap in the proximity region, $\Delta_1 \approx 0.7$ meV, and vanishing spin polarisation $P = 0$. Some contacts exhibit small non-zero values (see Fig. 3) of $P < 0.09(7)$, which may be a reflection of finite spin-splitting. The temperature dependence of the reflection is strong (as shown in Fig. 4), vanishing above $T > 5$ K, significantly lower that the $T_{\mathrm{c}} = 9.2$ K of the Nb tips used, likely due to the same proximity region of suppressed supercond. gap.

The magnetic field dependence of the PCAR spectra (see Fig. 5) is weak in fields of up to $\mu_0 H \leq 1.0$ T, with the

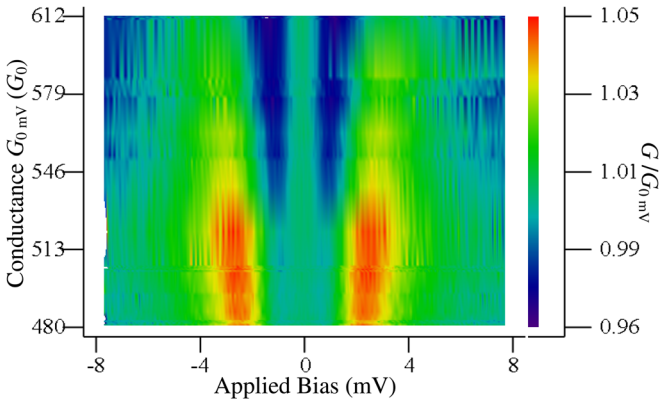

FIG. 1. Zero-bias conductance dependence (pressure, size, and barrier) of a Nb/Bi contact at $\mu_0 H = 0.0$ mT.

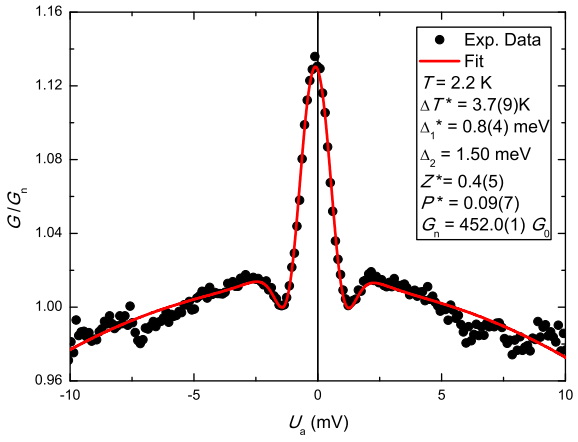

FIG. 3. A PCAR spectrum of a Nb/Bi contact at $T = 2.2$ K and $\mu_0 H = 0.0$ mT, exhibiting spin polarisation of 0.09(7).

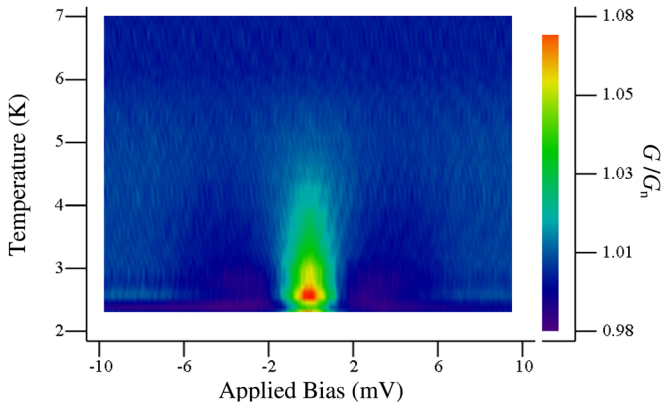

FIG. 4. Temperature dependence of the spectrum of a Nb/Bi contact at $\mu_0 H = 0.0$ mT and $G_n \approx 780\ G_0$.

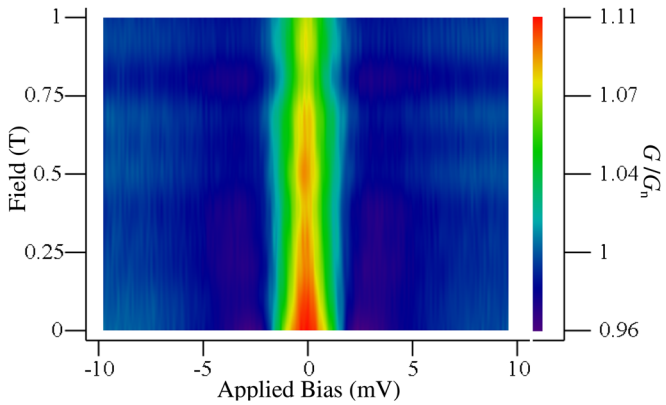

FIG. 5. Field dependence of the PCAR spectra of Nb/Bi contact at $T = 2.3$ K and $G_n \approx 780\ G_0$.

peak of the diff. conductance close to zero bias narrowing, instead of broadening on increasing field, understood in terms of the large field-induced suppression of the available DOS close to E_F, partially cancelling the effect of the magnetic field on the effective supercond. gap, and the supercond./normal fraction of the contact, broadening and lowering the DCS features.

It is useful to first address the possibility of a finite spin splitting of any of the carrier bands, present at the Fermi level, and therefore an existence of finite P close to E_F. As evidenced by Fig. 3, statistically, there could be finite spin polarisation of about $P = 0.09(7)$, developed at a particular crystallographic orientation of the Bi lattice with respect to the interface (the presented experiment cannot establish which one). This could be a result of a Mott-like SO scattering process, which a small amount of conduction electrons would undergo, because of significant SO coupling. This findings would appear to corroborate the observations of finite spin-polarisation at E_F, by spin-polarised and angle-resolved photoemission in Ref. 2. It must be mentioned that only a few percent of the observed DCS refine to non-zero values of P. The artefacts visible in Fig. 3, at biases above 4 mV, are likely due to inelastic scattering from phonons (a number of different acoustic and optical modes are available, with characteristic energies in the range of 4-13.5 meV).[14] Some DCS exhibit features reminiscent of three different carrier bands dispersing through the Fermi level (see Fig. 2). The absolute offsets are [0.12(3), 2.32(5), and 5.7(2)] meV, with corresponding FWHM widths of [2.9(2), 1.2(2), and 6.0(6)] meV. The band structure and the vicinity of E_F have been studied extensively by means of Shubnikov-de Haas (see, for example, Refs. 1, 15, and 16 and infrared magneto-reflectivity measurements[17] for pure bismuth and dilute alloys. The energy offsets of the first three Landau levels are reported to be (2.4, 4.51, and 5.88) meV in pure bismuth. The offset of E_F with respect to the bottom of the majority electron band is reported as 0.189(1) meV, and is somewhat higher than the offset observed here, likely due to the inferior impurity concentration in the polycrystalline sample used in the present study. The relative peak amplitudes observed, [16(1), 5(1), and 4.4(6)], agree approximately with the rough electron counts for the three main carrier bands (3, 1, 1).

The narrowing of the zero-bias PCAR peak (~0.5 meV/T) on increasing external magnetic field (see Fig. 5) is consistent with the magnetic field dependence of the band offset (with respect to E_F) for the light binary electrons, as verified in Ref. 17, of about 7.1 meV, with a slope of 0.47 meV/T. The above considerations suggest that the same methodology could be applicable to the characterisation of the electronic structure of other semimetals, such as graphite.

Useful discussions with J. M. D. Coey are gratefully acknowledged, as is financial support from Science Foundation Ireland, within the SSPP (11/SIRG/I2130) and NISE (10/IN1/I3002) programmes.

[1]L. S. Lerner, Phys. Rev. **127**, 1480 (1962).
[2]T. Hirahara, K. Miyamoto, I. Matsuda *et al.*, Phys. Rev. B **76**, 153305 (2007).
[3]P. Stamenov and J. M. D. Coey, J. Appl. Phys. **109**, 07C713 (2011).
[4]R. J. Soulen, J. M. Byers, M. S. Osofsky *et al.*, Science **282**, 85 (1998).
[5]I. I. Mazin, Phys. Rev. Lett. **83**, 1427 (1999).
[6]K. Gloos and F. Martin, Z. Phys. B **99**, 321 (1996).
[7]K. A. Yates, Y. Miyoshi, J. Grunwell *et al.*, J. Phys.: Conf. Ser. **97**, 012213 (2008).
[8]R. J. Soulen, M. S. Osofsky, B. Nadgorny *et al.*, J. Appl. Phys. **85**, 4589 (1999).
[9]G. E. Blonder, M. Tinkham, and T. M. Klapwijk, Phys. Rev. B **25**, 4515 (1982).
[10]P. Stamenov, J. Appl. Phys. **111**, 07C519 (2012).
[11]M. Stokmaier, G. Goll, D. Weissenberger, C. Sürgers, and H. v. Löhneysen, Phys. Rev. Lett. **101**, 147005 (2008).
[12]V. Baltz, A. D. Naylor, K. M. Seemann *et al.*, J. Phys.: Condens. Matter **21**, 095701 (2009).
[13]G. Sheet, S. Mukhopadhyay, and P. Raychaudhuri, Phys. Rev. B **69**, 134507 (2004).
[14]J. L. Yarnell, J. L. Warren, R. G. Wenzel, and S. H. Koenig, IBM J. Res. Dev. **8**, 234 (1964).
[15]L. S. Lerner, Phys. Rev. **130**, 605 (1963).
[16]H. T. Chv and Y.-H. Kao, Phys. Rev. B **1**, 2377 (1970).
[17]M. P. Vecchi, J. R. Pereira, and M. S. Dresselhaus, Phys. Rev. B **14**, 298 (1976).